THE STAR FORMATION NEWSLETTER
No.261 - 13 September 2014
2014/10/17

izumi natsuko (D2)

3-7

"Shocks in dense clouds. IV. Effects on grain-grain processing on molecular line emissions"
to
"Deuterated methanol in the pre-stellar core L1544"

Shocks in dense clouds

IV. Effects of grain-grain processing on molecular line emission

S. Anderi et al.　http://arxiv.org/pdf/1408.0140

Grain-grain process が C-type shockに与える影響

■ **Context**

・Grain-grain process : 高密度環境下のShockを考慮する上で非常に重要

■ **Aim**

・Grain-grain processの C-type shock への影響を調べる

1. 磁場の変化による影響は?
2. Molecular line emissionはどうなるか?
3. ↑特にshattering と vaporization による SiOのrotational line emission への影響は?

■ **Method**

Shattering、vaporizationの影響の詳細については
このシリーズの I - IIIの論文にあるとのこと

・2-fluid shock model

: Shattering と vaporization による影響を入れたmodel

: Multi-fluid modelを用いた計算より、ファクターで ~ 100倍早い

: LVG-based modelling を併せて用いる

■ Result

1. 磁場の変化による影響は?
   →磁場の幅広い値において、grain-grain processはC-type shockに強い影響を及ぼす
   ：Maximum temperatureは増加、shock widthは狭くなる
   →Grain-grain processの有無によって、Shock structureが磁場から受ける影響も変化する

2. Molecular line emissionはどうなるか?
   →Higher peak temperature により 高励起状態の分子増加
   →Lower shock width により柱密度減少
   →各分子やその遷移に対して、chemical / physical properties に影響を及ぼす

3. ↑特にshattering と vaporization による SiOのrotational line emission への影響は?
   →Vaporizationによってintensity増加するが、shock widthの減少により効果は相殺される
   →Intensityを増加するためには、SiOはgrain mantle中に存在することが必要となる

IRAM-30m large scale survey of ^{12}CO(2-1) and ^{13}CO(2-1) emission in the Orion molecular cloud

O. Berne et al. http://arxiv.org/pdf/1408.2999

Orion molecular cloudの広範囲・高解像度観測

■ Observation

- Telescope : IRAM 30 m telescope
- Region : 1 × 0.8° part molecular cloud
- Line : 12CO(2-1), 13CO(2-1)
- Maximum spatial resolution : ~ 11”
- Spectral resolution : 0.4 km s^{-1}

http://userpages.irap.omp.eu/~oberne/Olivier_Berne/Data

↑のページでデータ取得可能

■ Results

- Very clumpy and filamentary structure

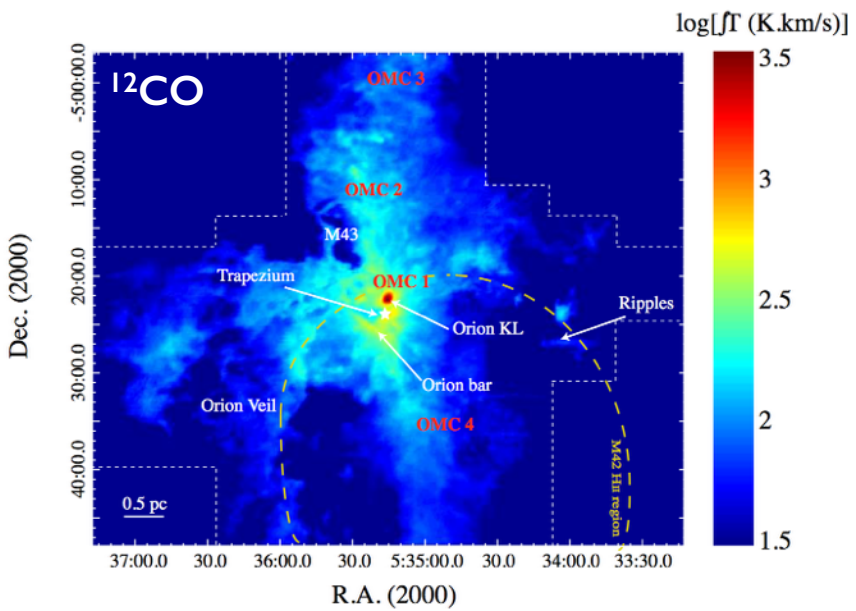

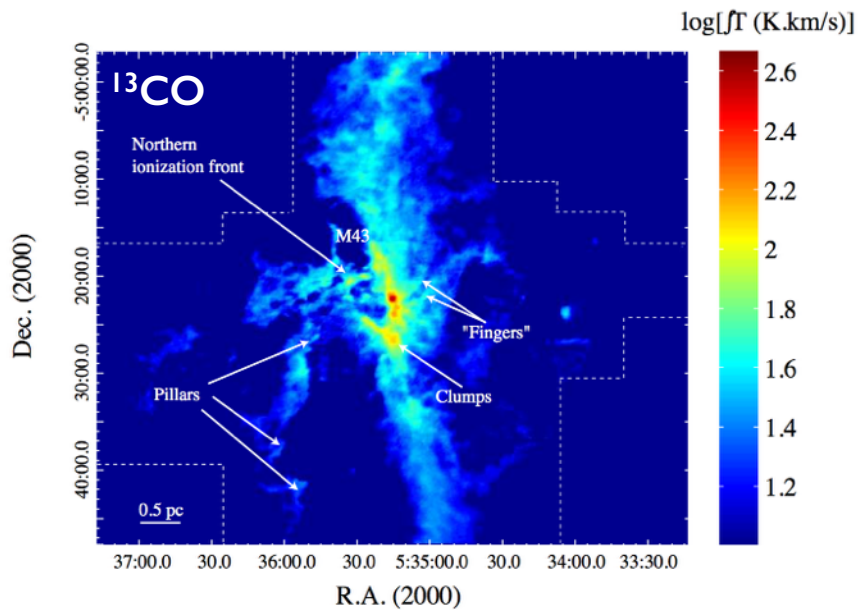

■ Properties

- Dynamical age : ~ 0.2 Myr
- Total mass : 7700 $M_\odot$

  ↑ 半分は “dense integral shaped filament”の内部

  もう半分は “filamentの周囲のmore diffuse and filamentary structure”に分布

- Total kinetic energy : 3.6×10^{40} J

  ↑ 40% : from the outflow

  60% : rest from the feedback of the HII region

  ※ただし場所による

  North region (OMC - 2/3) : outflow がdominant

  Center region (OMC - 1) : outflow / HII region 共にある

  South region : HII region がdominant

- Column density N_H

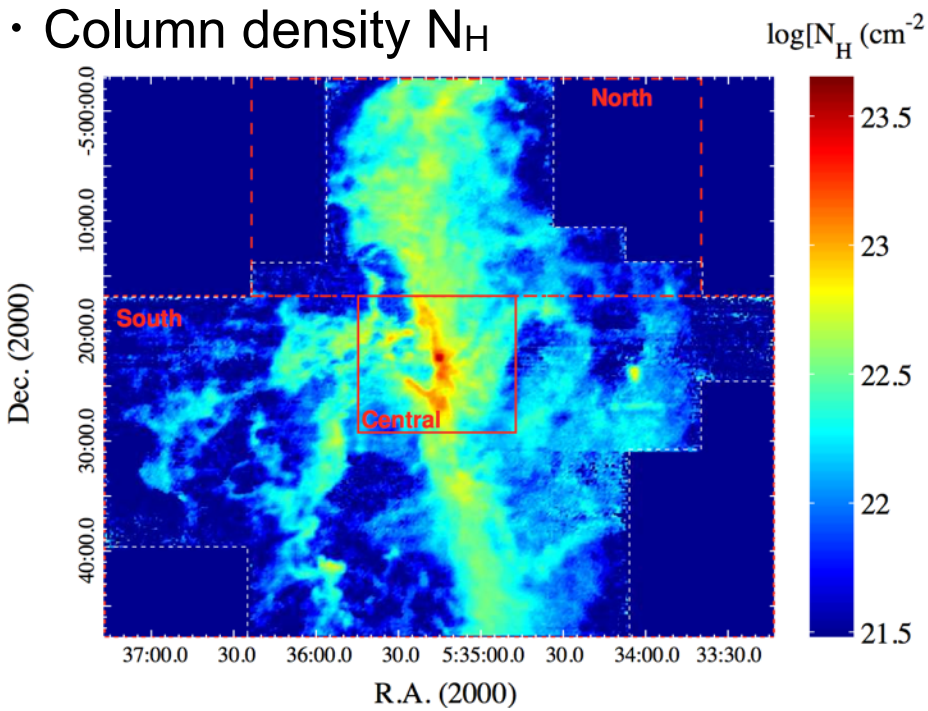

- South region の方が North regionより column density が小さいことが分かる

  → South regionでは星生成起こりづらい?

※実際に、South regionではprotostarの数が少ないことが確認されている

→ Orionではexpansion of HII regionによる triggered star formationはinefficientである

Table 1: Properties of the clumps in the Orion bar

Name	Position	Radius	Mass	Velocity dispersion	Virial paramater
Name	(R. A., Dec.) (deg.)	R_{clump} (")	M_{clump} ($M_\odot$)	δV (km/s)	α
Clump 1	(83.8075, -5.44827)	46.3	52.1	3.03	18.9
Clump 2	(83.8192, -5.43942)	23.4	13.6	2.08	17.3
Clump 3	(83.8431, -5.42102)	23.8	11.3	2.11	21.8
Clump 4	(83.8559, -5.41123)	14.7	4.30	2.12	35.6

Table 2: Derived parameters for the Orion molecular cloud

General parameters	
Total mass M	7700 $M_\odot$
Expansional velocity ΔV	10 km s^{-1}
Dynamical age τ_{dyn}	0.2 Myrs
Energy (Joules)	
Turbulent kinetic energy E_k	3.6×10^{40}
South region (OMC-4)	1.3×10^{40}
North region (OMC 2-3)	8.9×10^{39}
Central region (OMC 1)	1.4×10^{40}
... Orion bar	2.3×10^{39}
... Orion KL	1.1×10^{39}
... Molecular fingers	3.7×10^{39}
... Filamentary structures in the central region	6.5×10^{39}
Gravitational energy E_p	2.5×10^{41}
Thermal energy E_t	3.4×10^{39}
Magnetic energy E_B	$2 - 10 \times 10^{41}$
Starlight E_*	5×10^{44}

- Energy balance
  - Magnetic energy
    : Gravitational energy と同等かそれ以上
    : Kinetic energy より一桁大きい
  - Pressure
    : External pressure - order of a few 10^6 K.cm^{-3}
    : Magnetic pressure
      - Cloud周辺だとExternal pressureと同等だが、内部だと増加することが予想される

→全体的な結論として、magnetic fieldが分子雲を支える役割を主に担っていると考えられる

An Enigmatic Pointlike Feature within the HD 169142 Transitional Disk

Beth A. Biller et al. http://arxiv.org/pdf/1408.0794

HD 169142 transition disk でfaintなpointlike featureを検出

■ Target : HD 169142

- Nearly face-on transition diskをもつ
- 40-70 AUのannular gap検出されている

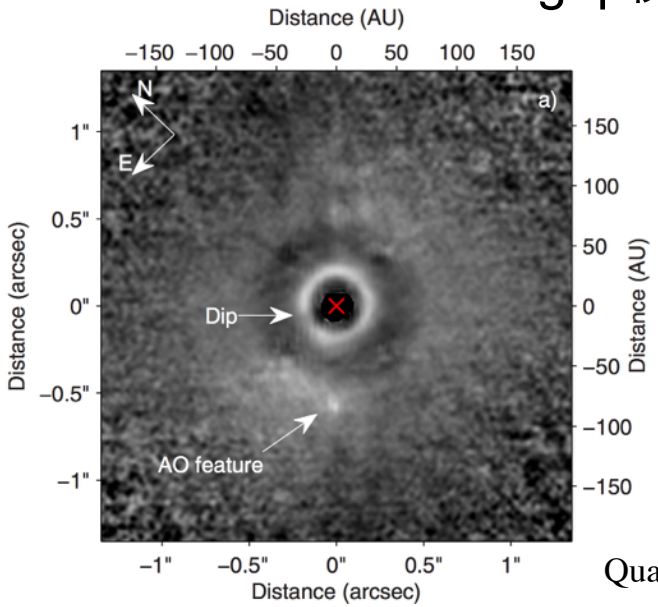

Quanz et al. 2013

Table 1. Properties of the HD 169142 System

	Primary	Disk Feature
Distance	145±10[a]	
Age	3-12 Myr[b]	
Proper Motion (μ_α, μ_δ)	(-2.1±1.5, −40.2±1.5) mas/yr[c]	
Separation: 14 July 2013 UT	···	0.11±0.03″ (∼16 AU)
Position Angle: 14 July 2013 UT	···	0±14°
$\Delta L'$	···	6.4±0.3
H (mag)	6.91[d]	···
Ks (mag)	6.41[d]	···
L' (mag)	5.64 [e]	12.0±0.3
$M_{L'}$ (mag)	-0.2	6.2±0.3
Spectral type	A7V[f]	···
Estimated Mass	1.65 $M_\odot$[f]	···

[a] Sylvester et al. (1996), but errors derived here.

[b] Grady et al. (2007)

[c] Høg et al. (2000)

[d] From 2MASS

[e] Malfait et al. (1998)

[f] Blondel & Djie (2006)

■ Observation

Table 2. Observation log

Telescope/Instrument	UT Date	Band	Exposure Time	Field Rotation
VLT NACO Vortex	14 July 2013	L'	75 min	135.2
MagAO CLIO-2 Narrow	9 April 2014	H	46 min	178.5
MagAO CLIO-2 Narrow	10 April 2014	H	30.4 min	172.9
MagAO CLIO-2 Narrow	12 April 2014	K_S	70 min	180.1
MagAO CLIO-2 Narrow	15 April 2014	3.9μm	60 min	164.1
MagAO VisAO Narrow	15 April 2014	z_p	82.4	176.8

■ Results

・Faint, pointlike feature を L' bandのデータで検出

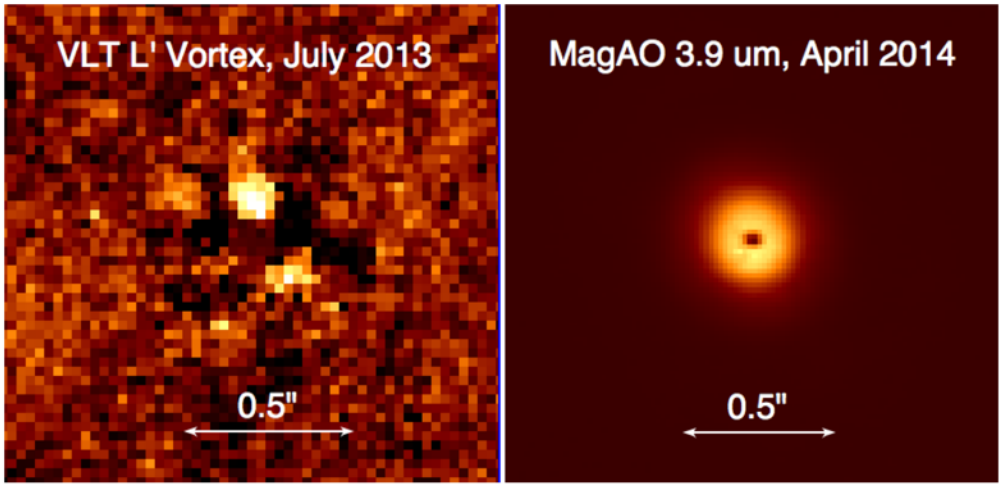

- Separation : ~ 0.11”
- Δmag (L) : ~ 6.4
- PA : ~ 0°

Fig. 1.— Left: L' July 2013 NACO Vortex image. We find a pointlike feature in the disk with Δmag=6.4±0.2, at a separation of 0.11±0.03″ and PA of 0±14°. Right: 3.9 μm April 2014 PSF-subtracted MagAO CLIO-2 image. Dark pixels in the core are due to saturation/non-linearity. The April 2014 MagAO image reached shallower contrasts than the original vortex image, hence the faint point-like feature is not retrieved. Our noncoronagraphic dataset was too shallow to retrieve the candidate (Δmag=5.6 at 0.11”).

↑ pointlike feature**検出**　　↑ pointlike feature**検出できていない**

↓位置関係はだいたいこんな感じ

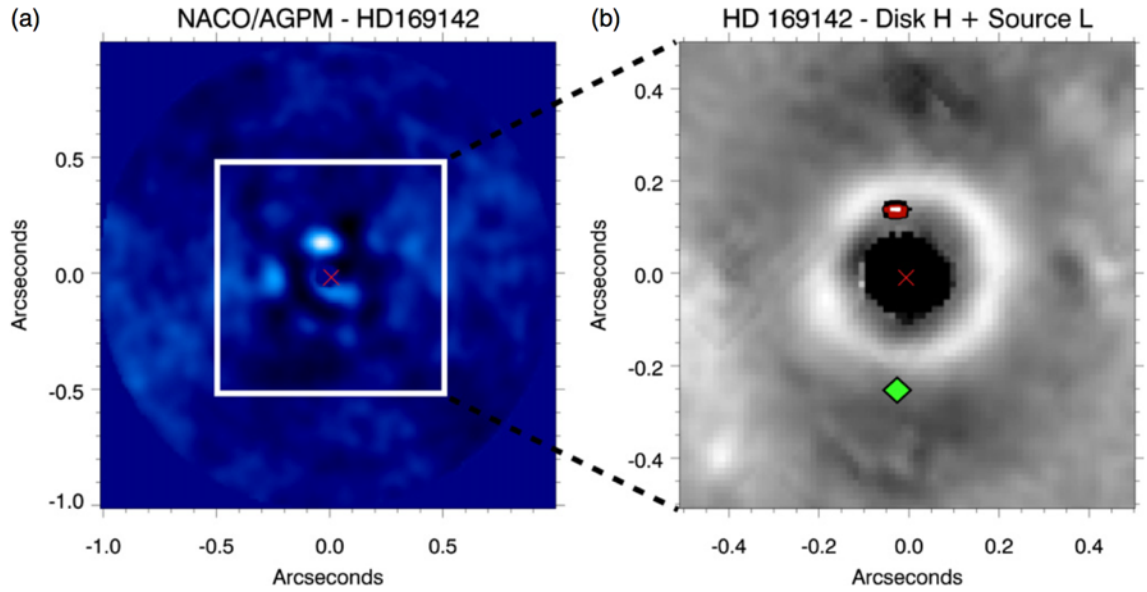

Reggiani et al. 2014

Figure 1. (a) NACO/AGPM L' image of HD 169142, using `PYNPOINT` with 20 PCA coefficients. A bright source is detected north of the central star. The image is scaled with respect to the maximum flux. (b) H-band PDI image of the circumstellar disk of HD 169142 (Quanz et al. 2013b). The inner cavity (<25 AU), the bright rim, and the annular gap (40–70 AU) are clearly visible. Overplotted in red contours is the detected L' source. The green diamond indicates the location of the compact 7 mm emission detected by Osorio et al. (2014).

・H, Ks bandでは検出されない

→ Photosphere of a substellar or mass companion によるものではない

→ Disk featureと考えられる

・L’ bandの検出

→ 強すぎてPassive heating from the starでは説明できない

→ Hαが検出されていない (Follette et al. in prep.) ため、accretionとも考えられない

・Pointlike featureの位置：disk gapの内側

→ Planet-formationに関連しているだろう

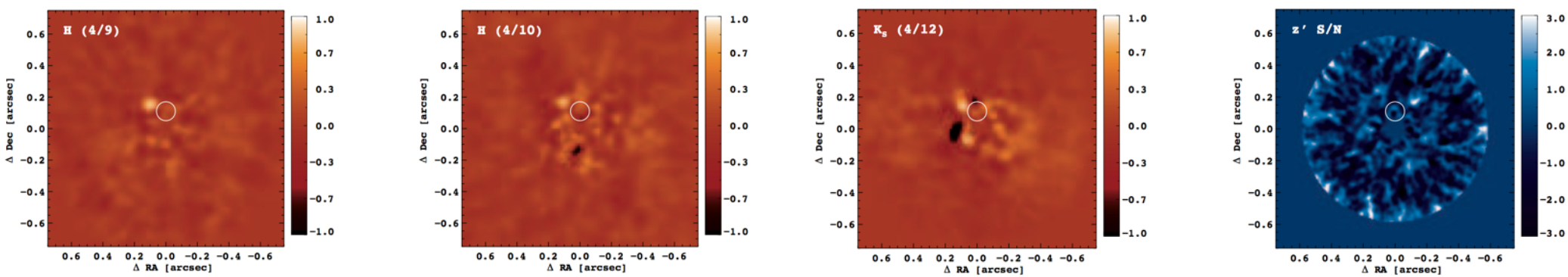

Fig. 2.— Top left and right : H band April 2014 MagAO CLIO-2 images over two consecutive nights, bottom left: K band April 2014 MagAO CLIO-2 image, bottom right: z’ band April 2014 MagAO VisAO image. All images have been reduced with PCA. The position of the L’ pointlike feature is circled.

今後の観測結果に期待する

Stellar irradiated discs and implications on migration of embedded planets III: viscosity transitions

Bertram Bitsch et al. http://arxiv.org/pdf/1408.1016

Viscosity transition による disk structure への影響

Small mass planet が恒星に落ち込む問題(落下問題) を解決したい

■ **Aims**

・Viscosity の α-parameterの急増による、disk structure への影響を調べる
→Disk の dead-zone structureのモデルを作成する

■ **Method**

・Focus on $\dot{M}$ disk (net mass flux が一定)

・Numerical hydrosimulations
: Explicit / implicit hydrodynamical code FARGOCA

■ **Results**

・Viscosity transition
: Surface density 変化する
→ Small planet の内側への移動を防ぐ (“Planet trap” mechanism)
この作用は$M_p > 0.5\ M_{Earth}$ まで働く
: 圧力勾配も変化する
→ Planetesimal formationを促進
ただしよりsteep (+ unrealistic) なtransitionが必要となる

Deuterated methanol in the pre-stellar core L1544

L. Bizzocchi et al. http://arxiv.org/pdf/1408.2491

L1544におけるCH_2DOHの観測

■ Aim

・L1544におけるmethanol deuterationの測定
→Deuterium fractionation processを調べる

■ Observation

・Telescope : IRAM 30 m telescope
・Line : CH_3OH, CH_2DOH, CH_3OD
・Mode : Single pointing (toward the L1544 dust emission peak)
Mapping (3'×3')

Table 1. Spectroscopic parameters of the observed methanol lines. Data are taken from Xu & Lovas (1997) for CH_3OH, from Pearson et al. (2012) for CH_2DOH, and from Anderson et al. (1988) for CH_3OD

Line	Rest frequency (MHz)	E_u/k_b (K)	g_u^a	A (10^{-5} s^{-1})
CH_3OH				
$2_{0,2} - 1_{0,1}, A^+$	96741.375	6.96	5	0.3408
$2_{1,2} - 1_{1,1}, E_2$	96739.362	12.53[b]	5	0.2558
$2_{0,2} - 1_{0,1}, E_1$	96744.550	20.08[b]	5	0.3407
$0_{0,0} - 1_{1,1}, E_1 - E_2$	108893.963	13.12[b]	1	1.471
CH_2DOH				
$2_{0,2} - 1_{0,1}, e_0$	89407.817	6.40	5	0.202
$3_{0,3} - 2_{0,2}, e_0$	134065.381	12.83	7	0.730
CH_3OD				
$1_{1,0} - 1_{0,1}, A^- - A^+$	133925.423	8.6	3	2.982

[a] Rotational degeneracy.
[b] Energy relative to the ground $0_{0,0}$, A rotational state.

■ Analysis

・Non-LTE modelling : Using the radiative transfer code MOLLIE (Keto & Rybicki 2010)

■ Results

・Mapping of CH_3OH : ピーク位置がdust continuumと異なる

→ Highly asymmetrical broken ring distribution

→ CO depletion holeの存在を示す

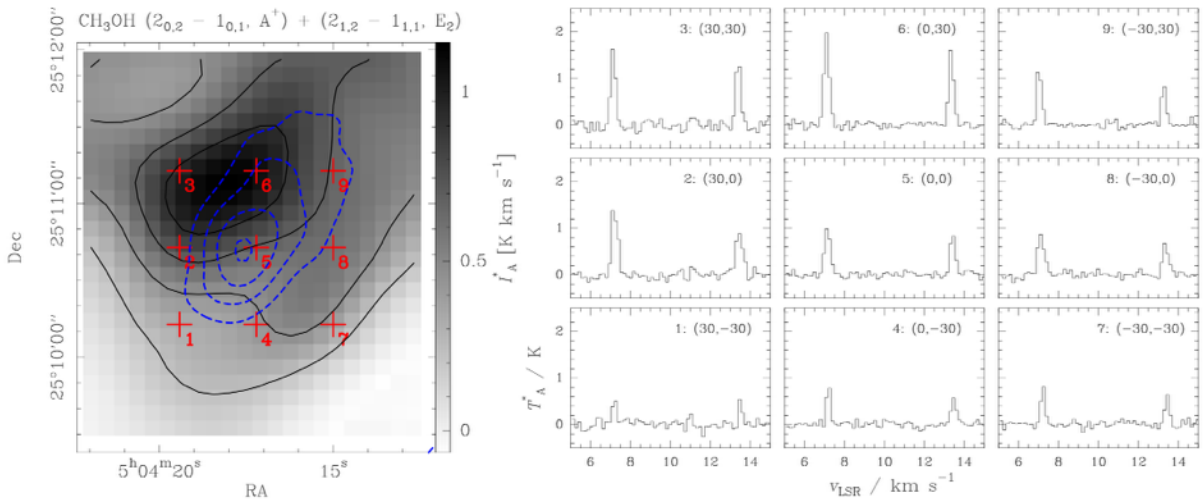

Fig. 2. (*Left panel*) Grey-scale map of the summed integrated intensity (units of T_A^*) of the $2_{0,2}-1_{0,1}$ (A^+) and $2_{1,2}-1_{1,1}$ (E_2) CH_3OH lines (30″angular resolution). Five equally spaced contours from 0.23 to 1.5 K km s^{-1} are plotted. The blue dashed contours plot the 1.3 mm continuum intensity map of Ward-Thompson et al. (1999) smoothed at 22″to improve the signal-to-noise ratio. Contours are at 100, 140, 180, and 220 mJy flux density levels. The red crosses represent the offset positions at which the spectra have been extracted. — (*Right panel*) Map spectra of the CH_3OH transitions towards the nine red crosses shown in the left panel. The velocity axis is centred on the $2_{0,2}-1_{0,1}$ (A^+) line at 7.2 km s^{-1}. The vertical axis of each spectrum represents the T_A^* scale in K, as shown in the lower leftmost panel.

・CH_3OH single-pointing

: $[CH_2DOH]$ / $[CH_3OH]$ = 0.10 ± 0.03

↑他の low-mass Class 0 protostarでの値より非常に小さい (0.4 - 0.6)

↑L1544の他の分子 (N_2H^+, NH_3, H_2CO..) での値よりも小さい

→Coreの外側 (CO just started to freeze out onto dust grains) を見ているのでは??

Caselli et al. 1999

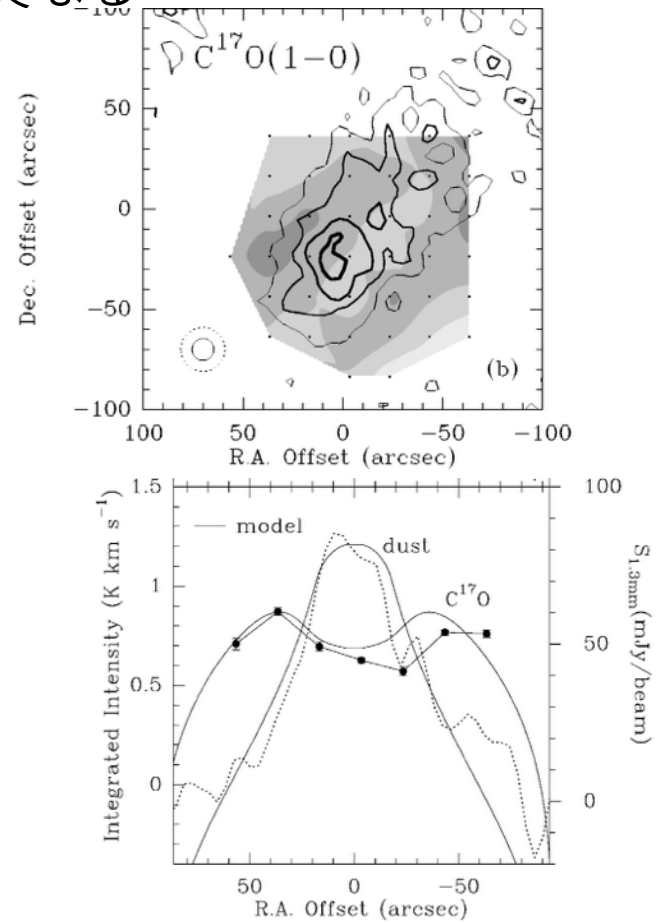

Table 2. Results of the CLASS GAUSS fit on the observed spectral profile of the methanol lines observed towards L1544. Numbers in parentheses refer to 3σ uncertainties in units of the last quoted digit.

Line	v_{LSR} (km s^{-1})	$\int T_A^* v$ (mK km s^{-1})	Δv (km s^{-1})
CH_3OH			
$2_{0,2}-1_{0,1}$ (A^+)	7.1804(11)	472.4(25)	0.3888(12)[a]
$2_{1,2}-1_{1,1}$ (E_2)	7.1808(14)	360.7(25)	0.3888(12)[a]
$2_{0,2}-1_{0,1}$ (E_1)	7.194(11)	43.0(20)	0.3888(12)[a]
$0_{0,0}-1_{1,1}$ (E_1-E_2)	7.1723(78)	67.1(30)	0.346(17)
CH_2DOH			
$(2_{0,2}-1_{0,1}, e_0)$	6.889(24)	30.5(42)	0.358(60)
$(3_{0,3}-2_{0,2}, e_0)$	6.939(22)	31.3(45)	0.313(48)

[a] Fitted as average value.